[Frontiers in Bioscience, Landmark, 21, 696-706, January 1, 2016]

Regulation of dynein-mediated autophagosomes trafficking by ASM in CASMCs

Ming Xu[1], Qiufang Zhang[1,2], Pin-Lan Li[1], Thaison Nguyen[3], Xiang Li[3], Yang Zhang[1,2,3]

[1]Department of Pharmacology and Toxicology, School of Medicine, Virginia Commonwealth University, Richmond, VA 23298, [2]Laboratory of Chinese Herbal Pharmacy, Renmin Hospital, Hubei University of Medicine, Shiyan, China, 442000, [3]Department of Pharmacological and Pharmaceutical Sciences, College of Pharmacy, University of Houston, Houston, TX 77204

TABLE OF CONTENTS

1. ABSTRACT

Acid sphingomyelinase (ASM; gene symbol Smpd1) has been shown to play a crucial role in autophagy maturation by controlling lysosomal fusion with autophagosomes in coronary arterial smooth muscle cells (CASMCs). However, the underlying molecular mechanism by which ASM controls autophagolysosomal fusion remains unknown. In primary cultured CASMCs, lysosomal Ca^{2+} induced by 7-ketocholesterol (7-Ket, an atherogenic stimulus and autophagy inducer) was markedly attenuated by ASM deficiency or TRPML1 gene silencing suggesting that ASM signaling is required for TRPML1 channel activity and subsequent lysosomal Ca^{2+} release. In these CASMCs, ASM deficiency or TRPML1 gene silencing markedly inhibited 7-Ket-induced dynein activation. In addition, 7-Ket-induced autophagosome trafficking, an event associated with lysosomal Ca^{2+} release and dynein activity, was significantly inhibited in ASM-deficient ($Smpd1^{-/-}$) CASMCs compared to that in $Smpd1^{+/+}$ CASMCs. Finally, overexpression of TRPML1 proteins restored 7-Ket-induced lysosomal Ca^{2+} release and autophagosome trafficking in $Smpd1^{-/-}$ CASMCs. Collectively, these results suggest that ASM plays a critical role in regulating lysosomal TRPML1-Ca^{2+} signaling and subsequent dynein-mediated autophagosome trafficking, which leads its role in controlling autophagy maturation in CASMCs under atherogenic stimulation.

2. INTRODUCTION

Autophagy is a tightly-controlled cellular catabolic pathway leading to lysosomal degradation and recycling of proteins and organelles in eukaryotes (1). It has been demonstrated that autophagy processes includes induction and formation of autophagosomes, autophagy maturation and autophagic efflux. During autophagy maturation, autophagosomes traffic and fuse with lysosomes, which leads to the acidification of autophagosomes to matured autophagolysosomes with acidic pH (2, 3). Autophagy maturation is a critical step in late stage of autophagy, which ensures efficient autophagic efflux, the process known as breakdown of autophagic contents in autophagolysosomes and autophagolysosomes themselves by lysosomal proteases (2, 3). Recent studies have indicated a protective role of autophagy in vascular smooth muscle cell (SMC) homeostasis during atherogenesis (4, 5).

In the vasculature of progressive atherosclerosis or restenosis after coronary angioplasty, moderately enhanced autophagy play a protective role by preventing an imbalance of vascular SMC homeostasis, which helps vascular smooth muscle in differentiated contractile phenotype, and thereby decreases cell proliferation and prevents fibrosis (6). In contrast, it is relatively understudied about the role of defective or reduced autophagy in the pathogenesis of atherosclerosis. In this regard, we recently demonstrated that impaired autophagy maturation causes defective autophagic efflux in acid sphingomyelinase (ASM; gene symbol *Smpd1*)-deficient coronary arterial SMCs (CASMCs), which is associated with enhanced protein expression of vimentin (a proliferative phenotype marker) and proliferation rate (7). Our studies for the first time implicated that impaired autophagy maturation may contributes to the pathogenesis of atherosclerosis via promoting SMC dedifferentiation and switching to a more proliferative phenotype. However, it remains unknown the precise mechanism how ASM signaling controls autophagy maturation process, particularly autophagosome trafficking, in CASMCs.

Upon autophagy induction, autophagosomes are formed in multiple sites in the cytoplasm, and these autophagosomes have to be trafficked and transported to meet with lysosomes. The precise molecular mechanisms underlying this transport process are not clear. Dynein ATPase is a multi-subunit microtubule motor protein complex, which is responsible for nearly all minus-end microtubule-based transport of vesicles within eukaryotic cells (8). A variety of intracellular motile processes are regulated by dynein ATPase activity including trafficking of membranous vesicles and other intracellular particles (9). This motor protein has been recently implicated in lysosomes and autophagosomes trafficking to meet and form autophagosomes (10, 11). Indeed, work in our laboratory has demonstrated that inhibition or loss of dynein function causes impaired autophagosome fusion with lysosomes, increased autophagosome accumulation, and reduced autophagolysosome formation in CASMCs (12). Previous studies have indicated that direct binding of Ca^{2+} to a component of the dynein complex regulates dynein motor function and its cytoplasmic distribution (13, 14). CD38 is a multifunctional enzyme responsible for the production and metabolism of a secondary messenger, NAADP (nicotinic acid adenine dinucleotide phosphate), in vascular cells (15). Mechanistically, NAADP can cause lysosomal Ca^{2+} release and thereby regulate lysosome function through its action on the transient receptor potential mucolipin-1 (TRPML1) channels, or through other mechanisms such as two-pore channels (16, 17). We recently demonstrated that CD38/NAADP-mediated lysosomal Ca^{2+} release plays an essential role in regulating dynein ATPase activity and autophagosome trafficking in CASMCs (12, 18). Therefore, based on these previous observations, we hypothesized that in ASM-deficient CASMCs under proatherogenic stimulation, inhibited dynein ATPase activation due to impaired lysosomal Ca^{2+} release via TRPML1 channels contributes to defective autophagosome trafficking leading to impaired autophagy maturation.

To test this hypothesis, we first determined whether the TRPML1-mediated lysosomal Ca^{2+} release response to proatherogenic stimulation is blunted in ASM-deficient CASMCs. Then, we examined whether dynein ATPase activation and autophagosomes trafficking in CASMCs with proatherogenic stimulation are also inhibited due to ASM deficiency. The roles of TRPML1 in lysosomal Ca^{2+} release, dynein activation and autophagosome trafficking in CASMCs are further confirmed by modulating its protein expression level by TRPML1 gene silencing or its cDNA overexpression.

3. MATERIALS AND METHODS

3.1. Mice

ASM-deficient (*Smpd1*$^{-/-}$; Smpd1 is the gene symbol for ASM gene, sphingomyelin phosphodiesterase 1) and wild-type (*Smpd1*$^{+/+}$) mice were used in the present study as we described previously (7, 19). All experimental protocols were reviewed and approved by the Animal Care Committee of Virginia Commonwealth University. All animals were provided standard rodent chow and water ad libitum in a temperature-controlled room.

3.2. Primary cell culture of mouse CASMCs

Mouse CASMCs were isolated as previously described (7, 20). In brief, mice were deeply anesthetized with intraperitoneal injection of pentobarbital sodium (25 mg/kg). The heart was excised with an intact aortic arch and immersed in a petri dish filled with ice-cold Krebs-Henseleit solution. A 25-gauge needle filled with Hanks' buffered saline solution was inserted into the aortic lumen opening while the whole heart remained in the ice-cold buffer solution. The opening of the needle was inserted deep into the heart close to the aortic valve. The needle was tied in place with the needle tip as close to the base of the heart as possible. The infusion pump was started with a 20 ml syringe containing warm HBSS through an intravenous extension set at a rate of 0.1. ml/min for 15 min. HBSS was replaced with warm enzyme solution (1 mg/ml collagenase type I, 0.5. mg/ml soybean trypsin inhibitor, 3% bovine serum albumin (BSA), and 2% antibiotic), which was flushed through the heart at a rate of 0.1. ml/min. Perfusion fluid was collected at 30, 60, and 90-min intervals. At 90 min, the heart was cut with scissors, and the apex was opened to flush out the cells that collected inside the ventricle. The fluid was centrifuged at 1000 rpm for 10 min, the cell-rich pellets were mixed with the media described below, and the cells were plated on 2% gelatin-coated six-well plates

and incubated in 5% CO_2 at 37°C. Advanced Dulbecco's modified Eagle's medium (DMEM) with 10% fetal bovine serum, 10% mouse serum, and 2% antibiotics were used for isolated CASMCs. The identification of CASMCs was based on positive staining by anti-α-actin antibody and the SMCs morphology. The medium was replaced 3 days after cell isolation and then once or twice each week until the cells grew to confluence. All studies were performed with cells of passage of 3-5. Six-week-old male C57BL/6J ASM-deficient ($Smpd1^{-/-}$) mice and their wild-type littermates ($Smpd1^{+/+}$) were used in the present study, and mouse genotyping was performed as we described previously (21).

3.3. Transfection of CASMCs with TRPML1 siRNA or cDNA plasmid

RNA interference of TRPML1 gene was achieved by transfection of double-stranded siRNA of targeting TRPML1 (Accession number: BC118374) consisted of 5'-CAGCUUCCGGCUCCUG-3' as we previously described (22). The scrambled small RNA (5′-AATTCTCCGAACGTGTCACGT-3′) was used as a negative control. Overexpression of TRPML1 was achieved by transfections of CASMCs with TRPML1 cDNA plasmids as described in our previous study (22, 23). Transfection of siRNA or cDNA was performed using the siLentFect Lipid Reagent or TransFectin Lipid Reagent (Bio-Rad, CA, USA) according to the manufacturer's instructions, as we described previously (24). The efficiency of TRP-ML1 silencing or overexpression in CASMCs was assessed by Western blotting as reported previously (22).

3.4. Fluorescent microscopic measurement of $(Ca^{2+})_i$ in CASMCs

A fluorescence image analysis system was used to determine $(Ca^{2+})_i$ in CASMCs with fura-2 acetoxymethyl ester (fura-2) as an indicator as previously described (17, 20), Having been loaded with 10 μM fura-2 at room temperature for 30 min, the cells were washed three times with Ca^{2+}-free Hank's buffer. The ratio of fura-2 emissions, when excited at the wavelengths of 340 and 380 nm, was recorded with a digital camera (Nikon Diaphoto TMD Inverted Microscope). Metafluor imaging and analysis software were used to acquire, digitize, and store the images for off-line processing and statistical analysis (Universal Imaging). The fluorescence ratio of excitation at 340 nm to that at 380 nm (F340/F380) was determined after background subtraction, and $(Ca^{2+})_i$ was calculated by using the following equation: $(Ca^{2+})_i = K_d\beta((R - R_{min})/(R_{max} - R))$, where K_d for the fura-2-Ca^{2+} complex is 224 nM; R is the fluorescence ratio (F_{340}/F_{380}); R_{max} and R_{min} are the maximal and minimal fluorescence ratios measured by addition of 10 μM of Ca^{2+} ionophore ionomycin to Ca^{2+}-replete solution (2.5. mM $CaCl_2$) and Ca^{2+}-free solution (5 mM EGTA), respectively; and β is the fluorescence ratio at 380-nm excitation determined at R_{min} and R_{max}, respectively. Lysosomal Ca^{2+} release was monitored indirectly by treating Fura-2-loaded CASMCs with Glycyl-L-phenylalanine 2-naphthylamide (GPN, 200 mM), a tripeptide causing osmotic lysis of cathepsin C–positive lysosomes.

3.5. Fluorescent confocal microscopic measurement of lysosome Ca^{2+} release

To detect lysosome Ca^{2+} release, sub-confluent CASMCs in 35-mm cell culture dishes were incubated with dextran-conjugated tetramethylrhodamine (Rho; 1 mg/ml; Molecular Probes) for 4 h in DMEM medium containing 10% FBS at 37°C, 5% CO_2, followed by a 20-h chase in dye-free medium for lysosomes loaded with Rho as previously described (12, 25). After being washed with Hank's buffered saline solution (HBSS) (in mM: 5.0. KCl, 0.3. KH_2PO_4, 138 NaCl, 4.0. $NaHCO_3$, 0.3. $Na_2HPO_4 \cdot 7H_2O$, 5.6. D-glucose, and 10.0. HEPES, with 2% antibiotics) three times, the Rho-loaded cells were then incubated with the Ca^{2+}-sensitive dye fluo-4 at a concentration of 5 μM. Ca^{2+} release and lysosome trace recordings were performed. Lysosome/Rho (Lyso/Rho) fluorescence images were acquired at 568-nm excitation and 590-nm emission. The co-localization coefficiency of Ca^{2+}/fluo-4 and Lyso/Rho was analyzed with Image-Pro Plus 6.0. software (26).

3.6. Assay of cytoplasmic dynein ATPase activity

Dynein in mouse CASMCs was purified using a published protocol with slight modification (18, 27). Cytoplasmic protein of mouse CASMCs was extracted with ice-cold extraction buffer (250 ml of 0.0.5 M PIPES-NaOH, 0.0.5 M HEPES, pH 7.0., containing 2 mM $MgC1_2$, 1 mM EDTA, 1 mM phenylmethylsulfonyl fluoride (PMSF), 10 μg/ml leupeptin, 10μg/ml tosyl arginine methyl ester (TAME), 1 μg/ml pepstatin A, and 1 mM dithiothreitol (DTT). Exogenous taxol (20 μM) was added to 20 mL of cell extract containing 4 mg/mL cytoplasmic protein, which was incubated in a 37°C water bath (with occasional swirling) for 12 min. The cell extract was underlayered with a prewarmed 7.5.% sucrose solution, and then centrifuged at 60,000 *g* for 30 min at 35°C. The supernatant was removed and the pellet was resuspended in 10 mL of extraction buffer containing 3 mM MgGTP and 5 μM taxol to release kinesin and dynamin. The resuspended pellet was incubated for 15 min prior to centrifugation at 60,000 *g* for 30 min. The supernatant was removed, and the pellet was resuspended in 1.2.5 mL of extraction buffer containing 10 mM Mg-ATP for 10 min at 37°C. The resuspended pellet was centrifuged at 200,000 *g* for 30 min at 25°C. The supernatant containing ATP-released cytoplasmic dynein was used for sucrose density gradient fractionation. Cytoplasmic dynein may constitute up to 50% of total protein in the ATP extract, the remainder consisting of tubulin and a low level of fibrous microtubule-associated proteins (MAPs). 1 mL ATP extract was further centrifuged on 10 mL of a 5-20% sucrose gradient in fractionation buffer (20 mM Tris-HCl,

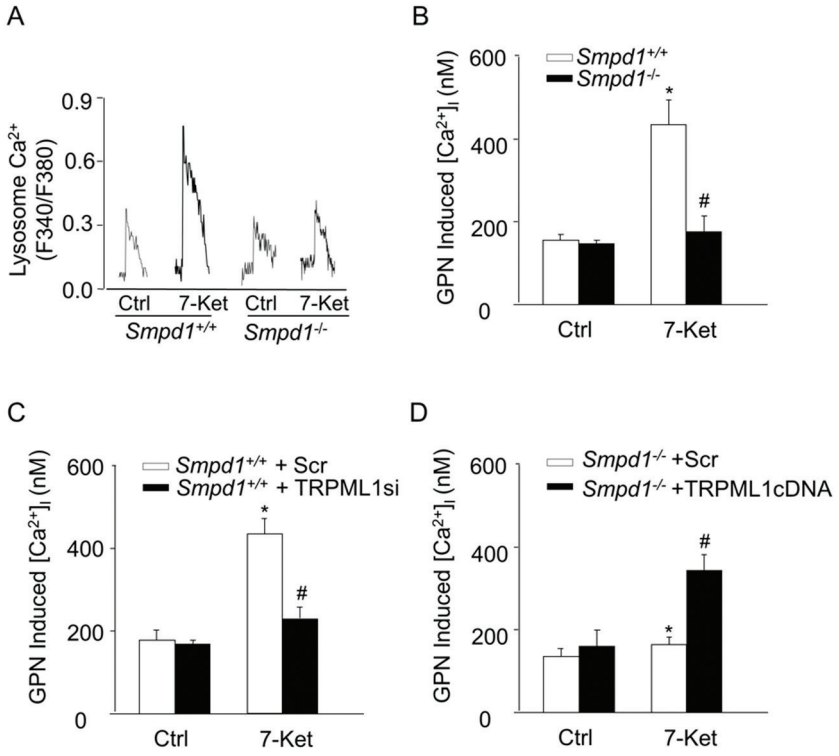

Figure 1. Lysosome Ca^{2+} release in response to proatherogenic stimuli in *Smpd1*$^{+/+}$ and *Smpd1*$^{-/-}$ CASMCs. Glycyl-l-phenylalanine-β-naphthylamide (GPN, 200 μM) was used to release Ca2+ from lysosomes. Representative lysosomal Ca2+ traces (A) and summarized data (B) showing the effects of *Smpd1* gene deficiency on GPN-induced lysosomal Ca^{2+} release in CASMCs (n=7). **P*<0.0.5 vs. Ctrl; #*P*<0.0.5 vs. *Smpd1*$^{+/+}$ CASMCs with 7-Ket (10 μM). (C) Effects of TRPML1 gene silencing using TRPML1 siRNA on GPN-induced lysosomal Ca^{2+} release in *Smpd1*$^{+/+}$ CASMCs (n=7). *P<0.0.5 vs. Ctrl; #*P*<0.0.5 vs. *Smpd1*$^{+/+}$ CASMCs Scr with 7-Ket. (D) Effects of TRPML1 gene overexpression using TRPML1cDNA on GPN-induced lysosomal Ca2+ release in *Smpd1*$^{-/-}$ CASMCs (n=7). *P<0.0.5 vs. Ctrl; #P<0.0.5 vs. *Smpd1*$^{-/-}$ CASMCs Scr with 7-Ket.

pH 7.6., 50 mM KCl, 5 mM $MgSO_4$, 0.5. mM EDTA and 1 mM DTT) at 125,000 *g* for 16 h at 4°C. Eleven 1 mL fractions were collected from the bottom of the tube. The dynein fraction peak at about fraction 5, well resolved from the other tubulin and MAPs.

The assays of dynein ATPase activity were performed in 50 μL reaction mixtures containing 20 mM Tris-HCl (pH 7.6.), 50 mM KCl, 5 mM $MgSO_4$, 0.5. mM EDTA and 1 mM DTT (28). In a standard assay condition, 10 μL of enzyme fractions and 4 mM of ATP were incubated with assay buffer at 37 °C for 40 min. The reaction was then stopped using highly acidic malachite green reagent and the absorbance was read at 660 nm in spectrophotometer (Elx800, Bio-Tek). The amount of inorganic phosphate release in the enzymatic reaction was calculated using the standard calibration curve generated with inorganic phosphate. The control in this assay contained all ingredients of the reaction mixture but the reaction was stopped at 0 time.

3.7. Dynamic analysis of autophagosome movement in CASMCs

CASMCs (2×10^4/ml) cultured in 35 mm dish were incubated with 12 μl BacMam GFP-LC3B virus particles at 37°C for 16 h to express the LC3B-GFP gene (18). The confocal fluorescent microscopic recording was conducted with an Olympus Fluoview System. The fluorescent images for autophagosomes (LC3B-GFP) of the CASMCs were continuously recorded at an excitation/emission (nm) of 485/520 by using XYT recording mode with a speed of 1 frame/10 second for 10 min. Vesicle tracking was performed in MAGEJ using the LSM reader and Manual tracking plugins according to the published protocol (11). Ten vesicles with GFP-LC3B were chosen at random for each cell. These vesicles were then tracked manually for as long as they were visible, while the program calculated velocities for each frame. All the results were further calculated and analyzed in Excel. The number of cells with different velocity of autophagosomes was calculated.

3.8. Statistics

Data are presented as means ± SE. Significant differences between and within multiple groups were examined using ANOVA for repeated measures, followed by Duncan's multiple-range test. Student's *t*-test was used to evaluate the significance of differences between two groups of observations. P < 0.0.5. was considered statistically significant.

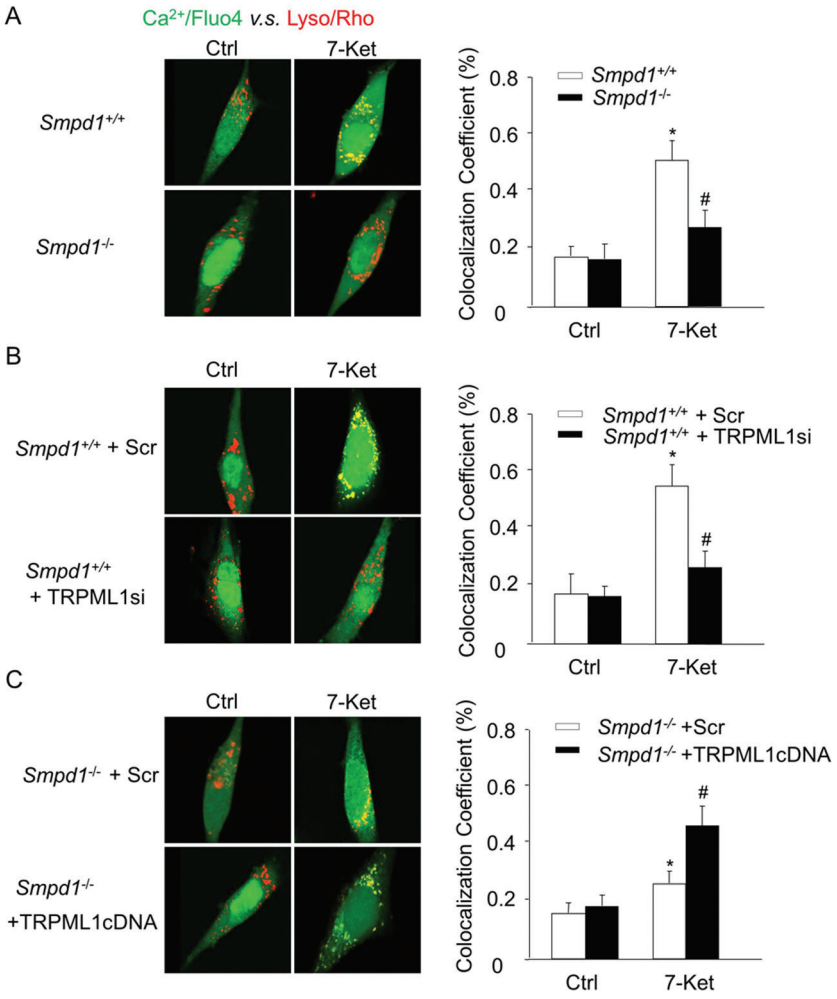

Figure 2. Confocal microscopic detection of Ca^{2+} release from lysosomes locally in *Smpd1*$^{+/+}$ and *Smpd1*$^{-/-}$ CASMCs. (A) Representative confocal microscopy images showing Ca^{2+} release regions that colocalized with lysosomes as shown by yellow spots formed by green fluo-4 signals with rhodamine-red lysosomal marker (Lyso/Rho). (B) Summarized data showing the effects of *Smpd1* gene deficiency on the colocalization coefficiency of Ca^{2+}/fluo-4 with Lyso/Rho signals (n=6). *P<0.0.5 vs. Ctrl; $^{\#}$P<0.0.5 vs. *Smpd1*$^{+/+}$ CASMCs with 7-Ket (10 μM). (C) Effects of TRPML1 gene silencing using TRPML1 siRNA on 7-Ket-induced colocalization of Ca^{2+}/fluo-4 with Lyso/Rho signals in *Smpd1*$^{+/+}$ CASMCs (n=6). *P<0.0.5 vs. Ctrl; $^{\#}$P<0.0.5 vs. *Smpd1*$^{+/+}$ CASMCs Scr with 7-Ket. (D) Effects of TRPML1 gene overexpression using TRPML1cDNA on 7-Ket-induced colocalization of Ca^{2+}/fluo-4 with Lyso/Rho signals in *Smpd1*$^{-/-}$ CASMCs (n=6). *P<0.0.5 vs. Ctrl; $^{\#}$P<0.0.5 vs. *Smpd1*$^{-/-}$ CASMCs Scr with 7-Ket.

4. RESULTS

4.1. Attenuation of 7-Ket-induced lysosomal Ca^{2+} release in *Smpd1*$^{-/-}$ CASMCs

To test whether impaired autophagy maturation in *Smpd1*$^{-/-}$ CASMCs was associated reduced lysosomal Ca^{2+} signaling, we conducted fluorescent imaging analysis to monitor lysosomal Ca^{2+} release by treating Fura-2 loaded CASMCs with 200 μM GPN. GPN was used to release Ca^{2+} from lysosomes by inducing their selective osmotic swelling. 7-Ketocholesterol (7-Ket) is a major oxidized cholesterol product and more atherogenic than cholesterol (29, 30). Since 7-Ket also induces autophagy process in SMCs (31), this oxidized cholesterol product (10 μM, 24 h treatment) was chosen as atherogenic stimulus in the present study as we reported recently (7). As shown in Figure 1A and 1B, GPN-induced Ca^{2+} release was significantly enhanced in *Smpd1*$^{+/+}$ CASMCs with 7-Ket stimulation, which was markedly attenuated in *Smpd1*$^{-/-}$ CASMCs. We recently reported that lysosomal Ca^{2+} release in CASMCs is primarily through the transient receptor potential mucolipin-1 (TRPML1) channels in lysosomes (16, 17). As shown in Figure 1C, we demonstrated that downregulation of TRPML1 by gene silencing blocked 7-Ket-enhanced lysosomal Ca^{2+} release in *Smpd1*$^{+/+}$ CASMCs, which indicates that TRPML1 mediates 7-Ket-enhanced lysosomal Ca^{2+} release in *Smpd1*$^{+/+}$ CASMCs. In contrast, overexpression of TRPML1 by its cDNA transfection markedly restored 7-Ket-enhanced lysosomal Ca^{2+} release in *Smpd1*$^{-/-}$ CASMCs (Figure 1D), which

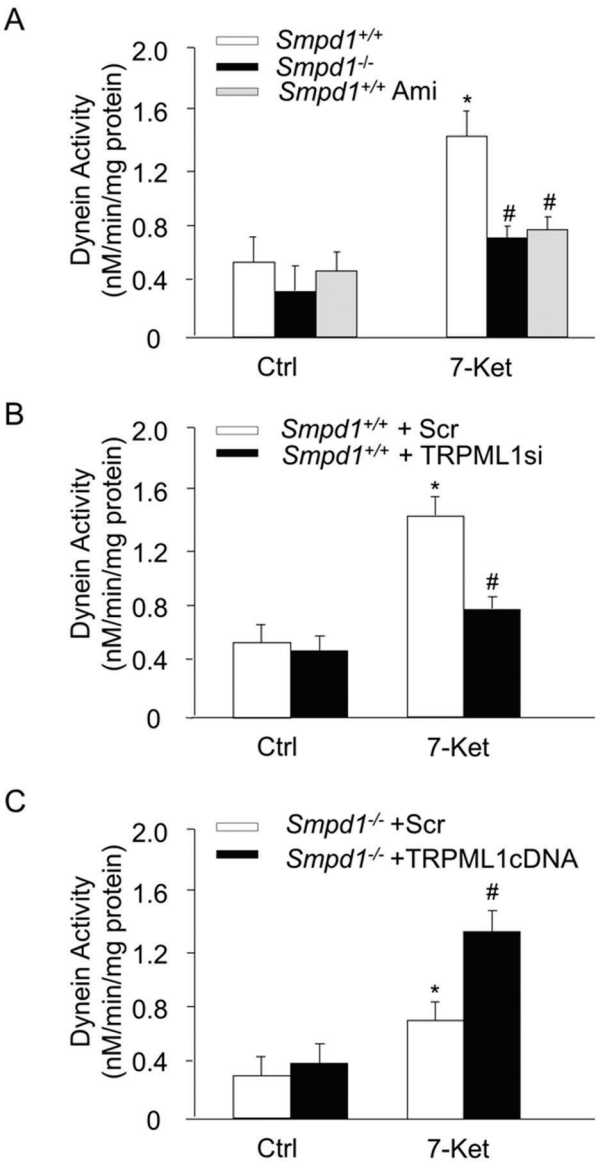

Figure 3. 7-Ket-induced dynein activation in *Smpd1*$^{+/+}$ and *Smpd1*$^{-/-}$ CASMCs. (A) Summarized data showing the dynein ATPase activity in *Smpd1*$^{+/+}$ and *Smpd1*$^{-/-}$ CASMCs or *Smpd1*$^{+/+}$ treated with amitriptyline (Ami, 1 μM) under control or with 7-Ket stimulation (n=6). *P<0.0.5 vs. Ctrl; $^{\#}$P<0.0.5 vs. *Smpd1*$^{+/+}$ CASMCs with 7-Ket. (C) Effects of TRPML1 gene silencing using TRPML1 siRNA on 7-Ket-induced dynein activity in *Smpd1*$^{+/+}$ CASMCs (n=6). *P<0.0.5 vs. Ctrl; $^{\#}$P<0.0.5 vs. *Smpd1*$^{+/+}$ CASMCs Scr with 7-Ket. (D) Effects of TRPML1 gene overexpression using TRPML1cDNA on 7-Ket-induced dynein activity in *Smpd1*$^{-/-}$ CASMCs (n=6). *P<0.0.5 vs. Ctrl; $^{\#}$P<0.0.5 vs. *Smpd1*$^{-/-}$ CASMCs Scr with 7-Ket.

suggests that TRPML1-meidated lysosomal Ca^{2+} release is impaired in *Smpd1*$^{-/-}$ CASMCs.

4.2. Decreased colocalization of Ca^{2+} regions with lysosomes in *Smpd1*$^{-/-}$ CASMCs

We further confirmed that lysosomal Ca^{2+} release is impaired in *Smpd1*$^{-/-}$ CASMCs by visualizing the lysosomal Ca^{2+} release locally in lysosomes, i.e. we measured the localization of Ca^{2+} around lysosomes by confocal microscopy after labeling cells with fluo-4. As shown in Figure 2A, the colocalization of Ca^{2+} release regions with lysosomes was indicated by yellow spots, which was formed by green fluo-4 signals with rhodamine-red lysosomal marker (Lyso/Rho). Quantification of the colocalization data revealed a significant increase in the colocalization coefficiency of fluo-4-Ca^{2+} and Lyso/Rho in in *Smpd1*$^{+/+}$ CASMCs when they were treated with 7-Ket. However, such colocalization of Ca^{2+} release regions with lysosomes by 7-Ket was markedly reduced in *Smpd1*$^{-/-}$ CASMCs. Similarly, we examined the effect of TRPML1 gene silencing or overexpression on the colocalization of Ca^{2+} regions with lysosomes in *Smpd1*$^{+/+}$ or *Smpd1*$^{-/-}$ CASMCs, respectively. As shown in Figure 2B, silencing of TRPML1 gene blocked 7-Ket-enhanced colocalization of Ca^{2+} release regions with lysosomes in *Smpd1*$^{+/+}$ CASMCs. As shown in Figure 2C, TRPML1 overexpression significantly restored 7-Ket-enhanced increases in the colocalization of Ca^{2+} release regions with lysosomes in *Smpd1*$^{-/-}$ CASMCs.

4.3. Inhibited dynein ATPase activation in *Smpd1*$^{-/-}$ CASMCs upon 7-Ket stimulation

Dynein is a motor protein responsible for nearly all minus-end microtubule-based transport of vesicles in eukaryotic cells. Recent studies have implicated this protein in autophagosomes trafficking to meet with the lysosomes to form autophagolysosomes, which is a critical step during autophagy maturation (2, 10, 11, 32, 33). We have also recently showed that dynein is involved in autophagosome trafficking in CASMCs (12). Thus, we examined whether ASM deficiency results in deregulated dynein activation during atherogenic stimulation. As shown in Figure 3A, treatment of CASMCs with 7-Ket resulted in a markedly increase in dynein ATPase activity in *Smpd1*$^{+/+}$ CASMCs, which was significantly attenuated in *Smpd1*$^{-/-}$ CASMCs or in *Smpd1*$^{+/+}$ CASMCs with ASM inhibitor amitriptyline. As shown in Figure 3B, silencing of TRPML1 gene blocked 7-Ket-induced dynein activation in *Smpd1*$^{+/+}$ CASMCs suggesting that TRPML1-mediated Ca^{2+} is the primary source of lysosomal Ca^{2+} release leading to dynein enhanced activation. As shown in Figure 3C, TRPML1 overexpression significantly restored 7-Ket-enhanced increases in the dynein activation in *Smpd1*$^{-/-}$ CASMCs, which further confirms that TRPML1-mediated lysosomal Ca^{2+} signaling controls dynein activity in CASMCs.

4.4. Inhibited autophagosome movement in *Smpd1*$^{-/-}$ CASMCs upon 7-Ket stimulation

We next examine whether reduced dynein activation contributes to impaired autophagosomes trafficking *Smpd1*$^{-/-}$ CASMCs. Autophagosomes are formed randomly throughout the cytoplasm and then transported to lysosomes. However, the majority of lysosomes are localized in the perinuclear region.

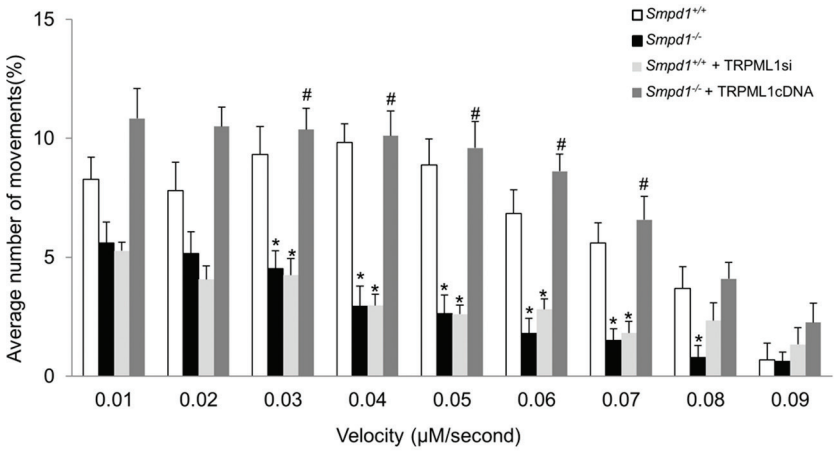

Figure 4. Analysis of autophagosome dynamic movements in 7-Ket stimulated *Smpd1*$^{+/+}$ and *Smpd1*$^{-/-}$ CASMCs. The summarized data show the velocity of autophagsomoes in 7-Ket stimulated *Smpd1*$^{+/+}$ and *Smpd1*$^{-/-}$ CASMCs, or in *Smpd1*$^{+/+}$ CASMCs with TRPML1 siRNA transfection as well as in *Smpd1*$^{-/-}$ CASMCs with TRPML1 cDNA transfection (n=6). *P<0.0.5 vs. Ctrl; #P<0.0.5 vs. *Smpd1*$^{+/+}$ CASMCs; #P<0.0.5 vs. *Smpd1*$^{-/-}$ CASMCs Scr with 7-Ket.

Therefore, autophagosomes need to be transported in the cytoplasm to meet and fuse with lysosomes. To monitor the autophagosomes movement to lysosomes, we labeled autophagosomes with LC3B-GFP by BacMam technique and determined the velocity of autophagosomes movement in *Smpd1*$^{+/+}$ and *Smpd1*$^{-/-}$ CASMCs with 7-Ket. As shown in Figure 4, autophagosomes movement was markedly reduced in the velocity-range between 0.0.1 mm/second and 0.0.9 mm/second in *Smpd1*$^{-/-}$ CASMCs compared to that in *Smpd1*$^{+/+}$CASMCs. Moreover, TRPML1 gene silencing has similar inhibitory effects to *Smpd1* gene deletion on autophagosome movement in *Smpd1*$^{+/+}$CASMCs, whereas overexpression of TRPML1 recovers the enhanced autophagosome movement in response to 7-Ket stimulation in *Smpd1*$^{-/-}$ CASMCs.

5. DISCUSSION

The purpose of the present study is to explore the roles of TRPML1-mediated lysosomal Ca^{2+} signaling and motor protein dynein in impaired autophagy maturation in ASM-deficient (*Smpd1*$^{-/-}$) CASMCs. In this study, we demonstrated that in CASMCs, ASM deficiency results in deregulated TRPML1-mediated lysosomal Ca^{2+} release signaling. Such impaired lysosomal Ca^{2+} signaling was associated with inhibited dynein activation and defective autophagosome trafficking in ASM-deficient CASMCs.

Accumulating evidence suggest that lysosome serves as another important intracellular Ca^{2+} store similar to the sarcoplasmic reticulum (34). Lysosomal Ca^{2+} can be released to mediate molecular trafficking or recycling and to control vesicular fusion events associated with lysosomes (35, 36). NAADP, a CD38-ADP-ribosylcyclase product, is one of the most potent intracellular Ca^{2+} mobilizing molecules, which mobilizes intracellular Ca^{2+} release in a two-pool mechanism depending upon a lysosome-dependent Ca^{2+} store in arterial SMCs (37, 38). Our previous studies have demonstrated that NAADP antagonist treatment markedly blocked 7-Ket enhanced lysosomal Ca^{2+} release response implicating a role of NAADP in mobilizing lysosomal Ca^{2+} in CASMCs upon proatherogenic stimulation (12). In the present study, we first observed that ASM deficiency abolished in 7-Ket enhanced lysosomal Ca^{2+} release in CASMCs by analyzing lysosomal Ca^{2+} release capacity using fura-2 fluorescence imaging. Further, we confirmed that ASM deficiency reduced colocalization of Ca^{2+} release regions with lysosomes by 7-Ket in CASMCs by directly visualizing the lysosomal Ca^{2+} release locally in lysosomes. Thus, our data for the first time reveal that in ASM-deficient CASMCs, lysosomal Ca^{2+} release response is impaired upon proathergenic stimulation. Together, the data from previous and present studies suggest that NAADP-mediated lysosomal Ca^{2+} release response is impaired in ASM-deficient CASMCs. Such impaired lysosome Ca^{2+} release response may be due to reduced numbers of lysosome Ca^{2+} stores via downregulation of lysosome biogenesis or increased lysosomal alkalizations (34). However, ASM deficiency did not alter either the number of lysosomes or expression of lysosome marker protein Lamp1 in CASMCs indicating that lysosome biogenesis remains unchanged in these ASM-deficient cells (7). Further, ASM deficiency had no effects on the lysosome acidic pH-dependent protease activity indicating that lysosomal pH is independent of ASM expression in CASMCs (7). Therefore, it seems that NAADP-mediated lysosomal release machinery is defective in ASM-deficient CASMCs. In vascular cells, NAADP-mediated regulation of lysosomal Ca^{2+} release and lysosome function is primarily through the activity of

the TRPML1 channels (16, 22). ASM is the key enzyme to hydrolyze sphingomyelin to ceramide in lysosomes and its deficiency commonly causes altered 'sphingolipid rheostat' with abnormal levels of sphingolipid species including sphingomyelin, ceramide, sphingosine and their phosphorylated metabolites (39), which can be major regulators for Ca^{2+}-dependent lysosomal trafficking function (40-42). A recent study has demonstrated that TRPML1-mediated lysosomal Ca^{2+} release is dramatically reduced in cells from Niemann-Pick disease patients (genetically deficient in *Smpd1* gene) (42), which is attributed to the inhibitory effects of sphingomyelin accumulation in lysosomal membranes by ASM deficiency on the TRPML1 channel activity. In the present study, we found that downregulation of TRPML1 expression by TRPML1 gene silencing mimics the inhibitory effect of ASM deficiency on 7-Ket enhanced lysosomal Ca^{2+} release, whereas overexpression of TRPML1 could restore the lysosomal Ca^{2+}release response in ASM-deficient cells. Therefore, similar inhibitory mechanism for TRPML1 activity may be present in ASM-deficient CASMCs.

One of important findings from the present study is that dynein activation in response to proatherogenic stimulation is inhibited in ASM-deficient CASMCs. To our knowledge, this is the first report showing that ASM controls dynein activity in mammalian cells. Dynein is a multi-subunit microtubule motor protein complex containing two identical heavy chains and the ATPase activity, which are responsible for generating movement of cargo along the microtubules. Previous studies have demonstrated that in mammalian cells, activation of this motor protein promotes nearly all minus-end microtubule-based transport of vesicles and more recently, lysosome and autophagosome trafficking (10, 11). Dynein activity inhibition or its function disruption abolishes lysosome fusion with autophagosomes and causes autophagosome accumulation in a variety of mammalian cells including glioma cells, neuronal cells, or SMCs (10, 12). Previous studies have reported that dynein motor function can be modulated by direct binding of Ca^{2+} to a component of the dynein complex, which causes redistribution of cytoplasmic dynein (13, 14). Therefore, dynein would be a potential target protein modulated by TRPML1-mediated lysosomal Ca^{2+} signaling. In the present study, 7-Ket enhanced dynein activity was blocked in ASM-deficient CASMCs. Similarly, transfection of wild-type CASMCs with TRPML1 siRNA also blocked dynein activation by 7-Ket, whereas TRPML1 overexpression corrected impaired dynein activation in ASM-deficient CASMCs. Thus, our data support the view that ASM controls TRPML1-mediated lysosomal Ca^{2+} signaling and subsequently modulates dynein activity in CASMCs upon proatherogenic stimulation.

Finally, we tested whether ASM deficiency impairs autophagosome trafficking and whether this process is regulated by TRPML1 activity. By quantifying the movement of LC3-GFP-labeled autophagosomes, we demonstrated that autophagosome movement within a cell was enhanced in 7-Ket treated *Smpd1*$^{+/+}$ CASMCs, which was markedly prevented in *Smpd1*$^{-/-}$ CASMCs (Figure 4). These results implicate that ASM function is needed for controlling autophagosome trafficking under proatherogenic stimulation. Deficiency of TRPML1 results in impaired lysosome trafficking and autophagolysosomal degradation in human fibroblasts (43). In the present study, we also demonstrated that silencing of the lysosomal Ca^{2+} channel TRPML1 mimics the inhibitory effects of ASM deficiency on 7-Ket-enhanced autophagosome trafficking in CASMCs. Moreover, TRMPL1 overexpression is sufficient to correct the defective autophagosome trafficking in *Smpd1*$^{-/-}$ CASMCs. Thus, these results indicate that defective autophagosome trafficking in *Smpd1*$^{-/-}$ CASMCs is a consequence of impaired TRPML1-mediated lysosomal Ca^{2+} signaling. Our data also support the view that upon atherogenic stimulation, ASM activity controls the TRPML1-mediated lysosomal Ca^{2+} release response and subsequent dynein-regulated autophagosome trafficking in CASMCs.

In summary, we for the first time link the impaired TRPML1-mediated lysosomal Ca^{2+} signaling due to ASM deficiency to the inhibited dynein activity and consequent defective autophagosome trafficking in CASMCs. Our study provides novel mechanistic insight about how ASM controls the autophagy maturation via regulating TRMPL1-mediated Ca^{2+} and dynein activity.

6. ACKNOWLEDGMENT

Ming Xu and Qiufang Zhang contributed equally and share first-authorship. This study was supported by grants from the National Institutes of Health (HL057244, HL122937 and HL122769) and National Natural Science Foundation of China (NO: 81303254).

7. REFERENCES

1. S. W. Ryter, S. J. Lee, A. Smith and A. M. Choi: Autophagy in vascular disease. *Proc Am Thorac Soc*, 7(1), 40-7 (2010) DOI: 10.1513/pats.200909-100JS
2. Z. Xie and D. J. Klionsky: Autophagosome formation: core machinery and adaptations. *Nat Cell Biol*, 9(10), 1102-9 (2007) DOI: 10.1038/ncb1007-1102
3. F. Reggiori and D. J. Klionsky: Autophagy in the eukaryotic cell. *Eukaryot Cell*, 1(1), 11-21 (2002) DOI: 10.1128/EC.01.1.11-21.2002
4. D. J. Klionsky and S. D. Emr: Autophagy as a regulated pathway of cellular degradation.

Science, 290(5497), 1717-21 (2000)
DOI: 10.1126/science.290.5497.1717

5. Y. M. Wei, X. Li, M. Xu, J. M. Abais, Y. Chen, C. R. Riebling, K. M. Boini, P. L. Li and Y. Zhang: Enhancement of autophagy by simvastatin through inhibition of Rac1-mTOR signaling pathway in coronary arterial myocytes. *Cell Physiol Biochem*, 31(6), 925-37 (2013)
DOI: 10.1159/000350111

6. P. Lacolley, V. Regnault, A. Nicoletti, Z. Li and J. B. Michel: The vascular smooth muscle cell in arterial pathology: a cell that can take on multiple roles. *Cardiovasc Res*, 95(2), 194-204 (2012)
DOI: 10.1093/cvr/cvs135

7. X. Li, M. Xu, A. L. Pitzer, M. Xia, K. M. Boini, P. L. Li and Y. Zhang: Control of autophagy maturation by acid sphingomyelinase in mouse coronary arterial smooth muscle cells: protective role in atherosclerosis. *J Mol Med (Berl)*, 92(5), 473-85 (2014)
DOI: 10.1007/s00109-014-1120-y

8. K. Oiwa and H. Sakakibara: Recent progress in dynein structure and mechanism. *Curr Opin Cell Biol*, 17(1), 98-103 (2005)
DOI: 10.1016/j.ceb.2004.12.006

9. R. Vallee: Molecular analysis of the microtubule motor dynein. *Proc Natl Acad Sci U S A*, 90(19), 8769-72 (1993)
DOI: 10.1073/pnas.90.19.8769

10. M. Yamamoto, S. O. Suzuki and M. Himeno: The effects of dynein inhibition on the autophagic pathway in glioma cells. *Neuropathology*, 30(1), 1-6 (2010)
DOI: 10.1111/j.1440-1789.2009.01034.x

11. L. Jahreiss, F. M. Menzies and D. C. Rubinsztein: The itinerary of autophagosomes: from peripheral formation to kiss-and-run fusion with lysosomes. *Traffic*, 9(4), 574-87 (2008)
DOI: 10.1111/j.1600-0854.2008.00701.x

12. M. Xu, X. X. Li, J. Xiong, M. Xia, E. Gulbins, Y. Zhang and P. L. Li: Regulation of autophagic flux by dynein-mediated autophagosomes trafficking in mouse coronary arterial myocytes. *Biochim Biophys Acta*, 1833(12), 3228-36 (2013)
DOI: 10.1016/j.bbamcr.2013.09.015

13. S. X. Lin and C. A. Collins: Regulation of the intracellular distribution of cytoplasmic dynein by serum factors and calcium. *J Cell Sci*, 105 (Pt 2), 579-88 (1993)

14. K. A. Lesich, C. B. Kelsch, K. L. Ponichter, B. J. Dionne, L. Dang and C. B. Lindemann: The calcium response of mouse sperm flagella: role of calcium ions in the regulation of dynein activity. *Biol Reprod*, 86(4), 105 (2012)
DOI: 10.1095/biolreprod.111.094953

15. E. G. Teggatz, G. Zhang, A. Y. Zhang, F. Yi, N. Li, A. P. Zou and P. L. Li: Role of cyclic ADP-ribose in Ca^{2+}-induced Ca^{2+} release and vasoconstriction in small renal arteries. *Microvasc Res*, 70(1-2), 65-75 (2005)
DOI: 10.1016/j.mvr.2005.06.004

16. F. Zhang, S. Jin, F. Yi and P. L. Li: TRP-ML1 functions as a lysosomal NAADP-sensitive Ca^{2+} release channel in coronary arterial myocytes. *J Cell Mol Med*, 13(9B), 3174-85 (2009)
DOI: 10.1111/j.1582-4934.2008.00486.x

17. F. Zhang, G. Zhang, A. Y. Zhang, M. J. Koeberl, E. Wallander and P. L. Li: Production of NAADP and its role in Ca^{2+} mobilization associated with lysosomes in coronary arterial myocytes. *Am J Physiol Heart Circ Physiol*, 291(1), H274-82 (2006)
DOI: 10.1152/ajpheart.01064.2005

18. Y. Zhang, M. Xu, M. Xia, X. Li, K. M. Boini, M. Wang, E. Gulbins, P. H. Ratz and P. L. Li: Defective autophagosome trafficking contributes to impaired autophagic flux in coronary arterial myocytes lacking CD38 gene. *Cardiovasc Res*, 102(1), 68-78 (2014)
DOI: 10.1093/cvr/cvu011

19. X. Li, W. Q. Han, K. M. Boini, M. Xia, Y. Zhang and P. L. Li: TRAIL death receptor 4 signaling via lysosome fusion and membrane raft clustering in coronary arterial endothelial cells: evidence from ASM knockout mice. *J Mol Med (Berl)*, 91(1), 25-36 (2013)
DOI: 10.1007/s00109-012-0968-y

20. M. Xu, Y. Zhang, M. Xia, X. X. Li, J. K. Ritter, F. Zhang and P. L. Li: NAD(P)H oxidase-dependent intracellular and extracellular O2*- production in coronary arterial myocytes from CD38 knockout mice. *Free Radic Biol Med*, 52(2), 357-65 (2012)
DOI: 10.1016/j.freeradbiomed.2011.10.485

21. K. M. Boini, M. Xia, C. Li, C. Zhang, L. P. Payne, J. M. Abais, J. L. Poklis, P. B. Hylemon and P.

L. Li: Acid sphingomyelinase gene deficiency ameliorates the hyperhomocysteinemia-induced glomerular injury in mice. *Am J Pathol*, 179(5), 2210-9 (2011)
DOI: 10.1016/j.ajpath.2011.07.019

22. M. Xu, X. Li, S. W. Walsh, Y. Zhang, J. M. Abais, K. M. Boini and P. L. Li: Intracellular two-phase Ca2+ release and apoptosis controlled by TRP-ML1 channel activity in coronary arterial myocytes. *Am J Physiol Cell Physiol*, 304(5), C458-66 (2013)
DOI: 10.1152/ajpcell.00342.2012

23. F. Zhang, M. Xu, W. Q. Han and P. L. Li: Reconstitution of lysosomal NAADP-TRP-ML1 signaling pathway and its function in TRP-ML1(-/-) cells. *Am J Physiol Cell Physiol*, 301(2), C421-30 (2011)
DOI: 10.1152/ajpcell.00393.2010

24. G. Zhang, F. Zhang, R. Muh, F. Yi, K. Chalupsky, H. Cai and P. L. Li: Autocrine/paracrine pattern of superoxide production through NAD(P)H oxidase in coronary arterial myocytes. *Am J Physiol Heart Circ Physiol*, 292(1), H483-95 (2007)
DOI: 10.1152/ajpheart.00632.2006

25. N. A. Bright, M. J. Gratian and J. P. Luzio: Endocytic delivery to lysosomes mediated by concurrent fusion and kissing events in living cells. *Curr Biol*, 15(4), 360-5 (2005)
DOI: 10.1016/j.cub.2005.01.049

26. V. Zinchuk, O. Zinchuk and T. Okada: Quantitative colocalization analysis of multicolor confocal immunofluorescence microscopy images: pushing pixels to explore biological phenomena. *Acta Histochem Cytochem*, 40(4), 101-11 (2007)
DOI: 10.1267/ahc.07002

27. B. M. Paschal, H. S. Shpetner and R. B. Vallee: Purification of brain cytoplasmic dynein and characterization of its *in vitro* properties. *Methods Enzymol*, 196, 181-91 (1991)
DOI: 10.1016/0076-6879(91)96018-M

28. S. Kumar, I. H. Lee and M. Plamann: Two approaches to isolate cytoplasmic dynein ATPase from Neurospora crassa. *Biochimie*, 82(3), 229-36 (2000)
DOI: 10.1016/S0300-9084(00)00206-6

29. M. A. Lyons and A. J. Brown: 7-Ketocholesterol. *Int J Biochem Cell Biol*, 31(3-4), 369-75 (1999)
DOI: 10.1016/S1357-2725(98)00123-X

30. N. Stadler, R. A. Lindner and M. J. Davies: Direct detection and quantification of transition metal ions in human atherosclerotic plaques: evidence for the presence of elevated levels of iron and copper. *Arterioscler Thromb Vasc Biol*, 24(5), 949-54 (2004)
DOI: 10.1161/01.ATV.0000124892.90999.cb

31. W. Martinet, D. M. Schrijvers, J. P. Timmermans and H. Bult: Interactions between cell death induced by statins and 7-ketocholesterol in rabbit aorta smooth muscle cells. *Br J Pharmacol*, 154(6), 1236-46 (2008)
DOI: 10.1038/bjp.2008.181

32. R. Kochl, X. W. Hu, E. Y. Chan and S. A. Tooze: Microtubules facilitate autophagosome formation and fusion of autophagosomes with endosomes. *Traffic*, 7(2), 129-45 (2006)
DOI: 10.1111/j.1600-0854.2005.00368.x

33. D. C. Rubinsztein, B. Ravikumar, A. Acevedo-Arozena, S. Imarisio, C. J. O'Kane and S. D. Brown: Dyneins, autophagy, aggregation and neurodegeneration. *Autophagy*, 1(3), 177-8 (2005)
DOI: 10.4161/auto.1.3.2050

34. K. A. Christensen, J. T. Myers and J. A. Swanson: pH-dependent regulation of lysosomal calcium in macrophages. *J Cell Sci*, 115(Pt 3), 599-607 (2002)

35. P. R. Pryor, B. M. Mullock, N. A. Bright, S. R. Gray and J. P. Luzio: The role of intraorganellar Ca(2+) in late endosome-lysosome heterotypic fusion and in the reformation of lysosomes from hybrid organelles. *J Cell Biol*, 149(5), 1053-62 (2000)
DOI: 10.1083/jcb.149.5.1053

36. E. Lloyd-Evans, H. Waller-Evans, K. Peterneva and F. M. Platt: Endolysosomal calcium regulation and disease. *Biochem Soc Trans*, 38(6), 1458-64 (2010)
DOI: 10.1042/BST0381458

37. J. M. Cancela, G. C. Churchill and A. Galione: Coordination of agonist-induced Ca^{2+}-signalling patterns by NAADP in pancreatic acinar cells. *Nature*, 398(6722), 74-6 (1999)
DOI: 10.1038/18032

38. A. Galione: NAADP, a new intracellular messenger that mobilizes Ca^{2+} from acidic stores. *Biochem Soc Trans*, 34(Pt 5), 922-6 (2006)
DOI: 10.1042/BST0340922

39. M. Taniguchi, K. Kitatani, T. Kondo, M. Hashimoto-Nishimura, S. Asano, A. Hayashi, S. Mitsutake, Y. Igarashi, H. Umehara, H. Takeya, J. Kigawa and T. Okazaki: Regulation of autophagy and its associated cell death by "sphingolipid rheostat": reciprocal role of ceramide and sphingosine 1-phosphate in the mammalian target of rapamycin pathway. *J Biol Chem*, 287(47), 39898-910 (2012) DOI: 10.1074/jbc.M112.416552

40. K. Glunde, S. E. Guggino, M. Solaiyappan, A. P. Pathak, Y. Ichikawa and Z. M. Bhujwalla: Extracellular acidification alters lysosomal trafficking in human breast cancer cells. *Neoplasia*, 5(6), 533-45 (2003) DOI: 10.1016/S1476-5586(03)80037-4

41. K. Trajkovic, A. S. Dhaunchak, J. T. Goncalves, D. Wenzel, A. Schneider, G. Bunt, K. A. Nave and M. Simons: Neuron to glia signaling triggers myelin membrane exocytosis from endosomal storage sites. *J Cell Biol*, 172(6), 937-48 (2006) DOI: 10.1083/jcb.200509022

42. D. Shen, X. Wang, X. Li, X. Zhang, Z. Yao, S. Dibble, X. P. Dong, T. Yu, A. P. Lieberman, H. D. Showalter and H. Xu: Lipid storage disorders block lysosomal trafficking by inhibiting a TRP channel and lysosomal calcium release. *Nat Commun*, 3, 731 (2012) DOI: 10.1038/ncomms1735

43. S. Vergarajauregui, P. S. Connelly, M. P. Daniels and R. Puertollano: Autophagic dysfunction in mucolipidosis type IV patients. *Hum Mol Genet*, 17(17), 2723-37 (2008) DOI: 10.1093/hmg/ddn174

Abbreviations: 7-Ket: 7-ketocholesterol, ASM: acid sphingomyelinase, CASMC: coronary arterial smooth muscle cell, GPN: Glycyl-L-phenylalanine 2-naphthylamide, NAADP: Nicotinic acid adenine dinucleotide phosphate, Smpd1: sphingomyelin phosphodiesterase 1, TRPML1: transient receptor potential mucolipin-1

Key Words: Smooth Muscle Cells, Autophagy Maturation, Sphingomyelinase, Lysosomal Ca^{2+}

Send correspondence to: Yang Zhang, Department of Pharmacological & Pharmaceutical Sciences, College of Pharmacy, University of Houston, Houston, TX 77204, Tel: 713-743-7710, Fax: 713-743-1259, E-mail: yzhan219@central.uh.edu